Status report on the DESIR facility
SPIRAL2 SAC meeting à Giens, June 9, 2008

Following the Letter of Intent submitted by a large international collaboration to the SPIRAL2 SAC, the construction of the DESIR facility has been strongly recommended by the SPIRAL2 SAC. Due to this support, the detailed design of the DESIR building was included in the design studies of the other SPIRAL2 buildings, which are the accelerator building, the AEL building(s), both of which form the phase 1 of the construction plans, as well as of the production and the DESIR building, which form phase 2.

The DESIR hall

Following this logic, the DESIR collaboration works presently with the SPIRAL2 Civil construction department in order to define the detailed construction programme and to precisely work out the interfaces between the different buildings. The DESIR facility will consist of the main experimental hall, the RFQ-HRS room which is part of the SPIRAL2 production building, 15 technical rooms (workshop, grey rooms, assembly rooms, supply rooms, control etc), a meeting room, a DAQ and control room, and a kitchen. All needs for these different rooms have been identified and defined. In addition, a general layout-scheme of the DESIR hall was sketched for the first time evidencing the need for a building size of the order of 1500m^2. Drawings of the DESIR hall and its basement are shown in the following figures.

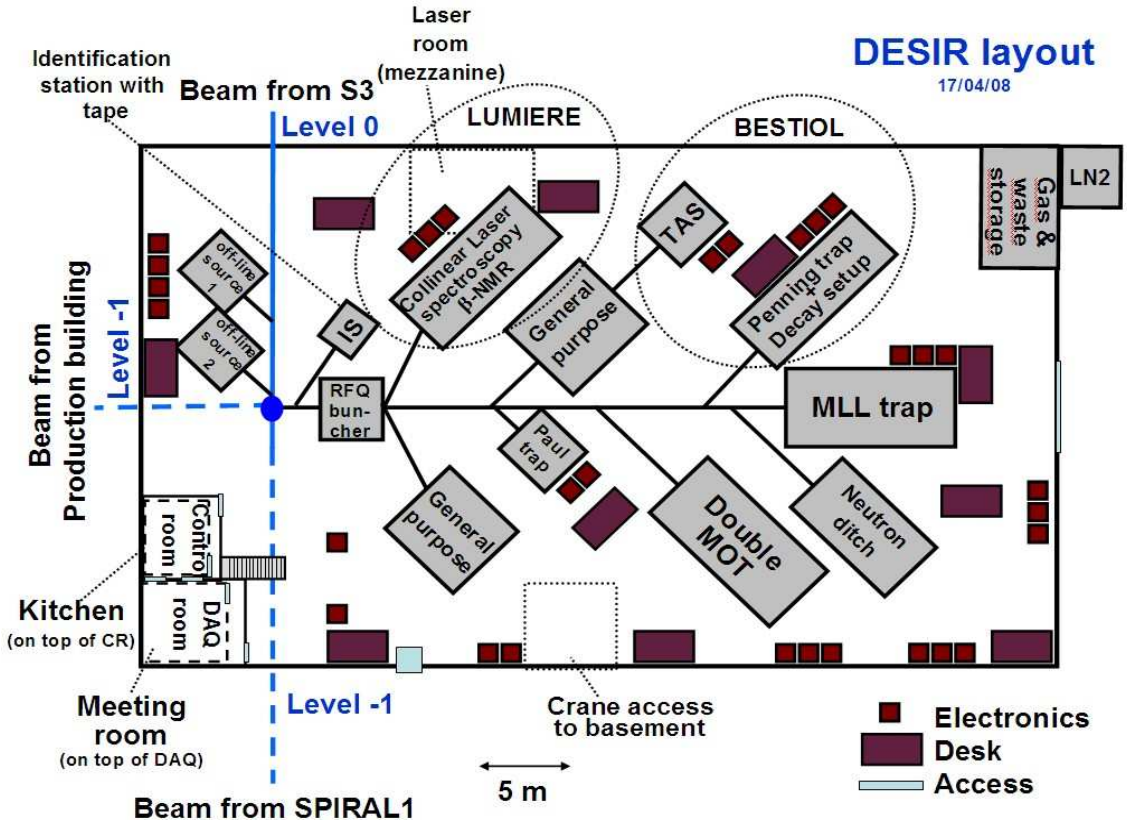

Figure 1: General layout of the DESIR experimental hall. The figure shows a possible arrangement of the different permanent installations, the general purpose areas as well as of the meeting, control, DAQ rooms and the kitchen.

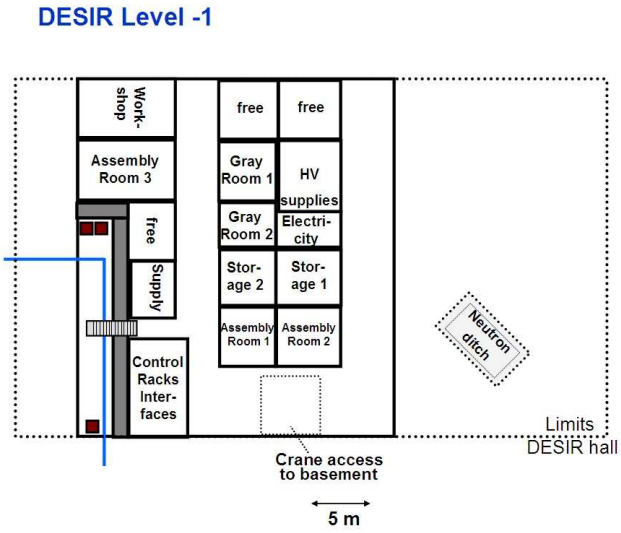

Figure 2: Possible arrangement of the different technical rooms of DESIR, most likely in the basement of the DESIR hall.

The RFQ cooler and the HRS

Work is also ongoing on the design of the DESIR HRS and the RFQ cooler SHIRAC, which will cool beams before injection in the HRS. As for the RFQ, measurements with the prototype of the RFQ cooler have started at the LPC Caen. For the first time, beams could be transmitted through the system, however, for the moment with low transmission. Modifications to the present system are on the way to improve on this. In addition, the development of the HF system and the coupling HF-DC has been finished. For the first time, 300 W have been generated, which corresponds to 2.2kV_{pp} at 6 MHz for the RFQ. A future upgrade top 600 W is foreseen for the future. High-voltage and pressure tests have been performed also successfully to see whether sparking problems could limit the HV and pressure regimes foreseen. No important limitation was found within the running regime of the RFQ.

A detailed ion optical design of the HRS was performed at the CENBG. Its was decided that we adopt a solution very close to, if not exactly as, the design of the HRS of the CARIBU project at Argonne National Laboratory. Details of these studies are given in the preliminary version of a report attached to this document. The general layout of the RFQ and the HRS are given in the following figure.

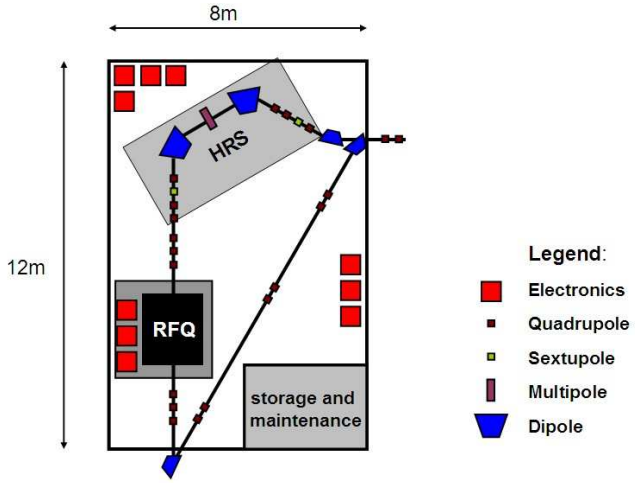

Figure 3: Layout of the RFQ-HRS room in the SPIRAL2 production building. A beam line by-passing the RFQ and the HRS is also foreseen.

Beam line from S3 to DESIR

S3 with its low-energy branch consisting of a gas catcher and a dipole magnet will produce radioactive isotopes at ISOL energies. In contrast to the standard productions scheme of SPIRAL2 which works with solid catchers where the production strongly depends on the chemistry of the element to be produced, the low-energy branch of S3 will produce any radioactive nuclide as long as the production rate is reasonably high.

At the last SPIRAL2 SAC meeting, the S3 and DESIR collaborations proposed the construction of a beam line from S3 to DESIR in order to use the ISOL beams from S3 with the ISOL equipment which will be installed in the DESIR facility. The strong support which this option got from the SPIRAL2 SAC triggered a re-arrangement of the different buildings of SPIRAL2 in order to facilitate the coupling of S3 and DESIR.

Collaborative work has continued in this sense, in particular for the technical proposal of S3, where part of the physics case deals with experiments which will be performed in DESIR with beams produced at S3.

Safety at DESIR

Another topic on which work has started in close collaboration with people from GANIL is the safety requirements in DESIR. The main topics of concern are the intensity limitations necessary to keep the DESIR hall a “green” area, which means that the hall is accessible while the beam is delivered to one of the DESIR installations. In particular, we have to define how safety requirements can be implemented and verified permanently. Another question is also whether the different setups have to be defined as caves, i.e. surrounded by concrete or whether they can be kept completely open as e.g. at ISOLDE.

For this purpose ‘limiting cases’ calculations are underway to see whether for each mass or isotope the full beam intensity can be given to DESIR, under which conditions, or whether intensity cuts have to be imposed.

DESIR web pages

As a means of communication and diffusion of information, the DESIR web pages have been put online recently. They contain information on the physics at DESIR, the facility layout, the experimental equipment which will be installed at DESIR, information on the DESIR collaboration, and much more. They can be found at www.cenbg.in2p3.fr/desir

Future activities

The main activity in the near future will be to finalise within the SPIRAL2 project the construction program for DESIR. This includes not only the civil construction, but also all necessary supplies for the different setups in the DESIR hall and any other requirements to facilitate the installation of equipment and the use of the DESIR facility.

In parallel, the tests of the prototype RFQ will continue to end up by the end of 2008 with a technical design for the DESIR RFQ SHIRAC.

The optical study of the HRS will continue in particular to refine the precision requests in terms of manufacturing and misalignment. A possible collaboration with Argonne National laboratory is under discussion for some of the technical aspects.

Details of the safety procedures, of the radioprotection scheme in DESIR, of possible radioactive beam intensity limitations in order to keep the DESIR hall as a “green” zone will be worked out in the near future as well.

With this work done, we will converge towards a technical proposal in the next one or two years.

APPENDIX

TECHNICAL REPORT

DESIR HIGH RESOLUTION SEPARATOR

TERESA KURTUKIAN NIETO

CEN BORDEAUX-GRADIGNAN

MAY 28TH , 2008

PRELININARY VERSION

TECHNICAL REPORT

DESIR HIGH RESOLUTION SEPARATOR (HRS)

OVERVIEW

The extracted isotopes from SPIRAL2 will be transported to and cooled in a RFQ cooler yielding beams with very low transverse emittance and energy spread. These beams will then be accelerated to 60 keV and sent to a high-resolution mass separator (HRS) where a specific isotope will be selected. The good beam properties extracted from the RFQ cooler will allow one to obtain a mass resolution of ~20000 with the HRS.

HRS: LATTICE STRUCTURE AND MAGNETS

TECHINICAL REQUIREMENTS

1. High transmission (ideally close to 100%) and high resolving power ($m/\Delta m$ ~20000) to provide monoisotopic beams of exotic nuclides.
2. Match beam emittance from RFQ cooler ($\varepsilon < 3\pi$ mm-mr, $\Delta E < 1$ eV at 60 keV)
3. Compact configuration. Must fit in the SPIRAL2 production building (12 m x 8 m)
4. Should be robust in order to tolerate errors in alignment and component manufacturing.
5. Cheep, concerning both installation and operation costs.

ION-OPTICAL DESIGN CONCEPT

The ion optical design of the separator is presented in Figure 1. The proposed design will consists of two 60 degree magnetic dipoles (D) with 23º entrance and exit angles, four matching quadrupoles (MQ), two focusing quadrupoles (FQ), two focusing sextupoles (FS) and one multipole (M) with the configuration QQSQDMDQSQQ. The optical axis has a length of 6.9m, measured from the first to the last quadrupole. The HRS is mirror symmetric with respect to the mid-plane to minimise aberrations.

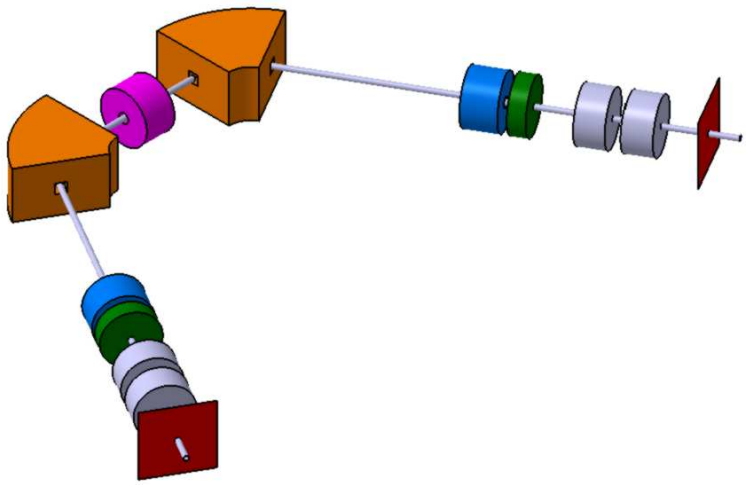

Figure 1. 3D layout of the DESIR HRS consisting of two matching quadrupole doublets (grey), two focusing sextupoles (green), two focusing quadrupoles (blue), two 60 degree dipoles and one multipole (pink).

Quadrupoles are used as the focusing mode in the y-direction and defocusing in x-direction. This offers two advantages simultaneously: high transmission as well as small image magnification to attain high resolution. The first quadrupole doublet produces a ribbon-shaped beam, so y angles are small minimising y angle aberrations. The quadrupole placed before the dipole diverges in x-direction and converges in y-direction. The small y size minimises y aberrations and the large x area in the dipoles gives mass dispersion. The reverse matching section transforms the ribbon-shaped beam back to a circular cross section at the focal plane. The two sextupoles and the central multipole (sextupole, octupole, decapole and duodecapole) allow correcting aberrations to 5th order. The explicit information about the exact location of the different elements and the corresponding sizes are summarised in Figure 2 and tables 1, 2 and 3.

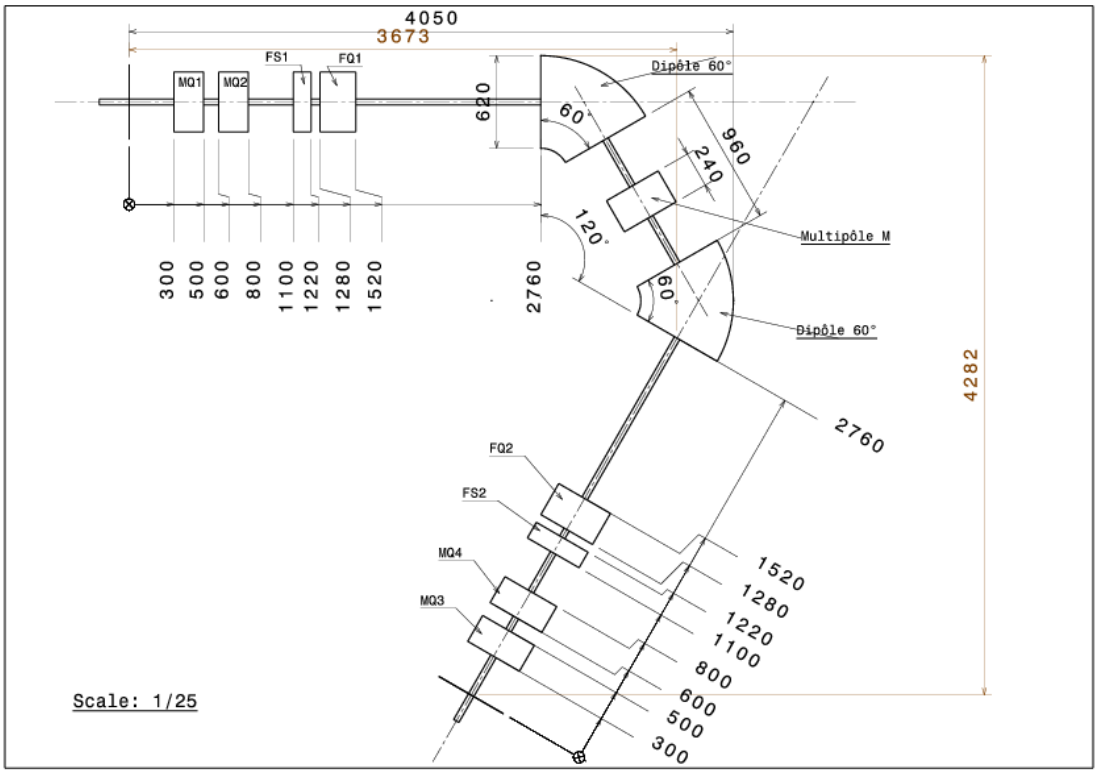

Figure 2 Detailled scheme of the HRS

Table 1.Lattice configuration

Element	Length (mm)	Element	Length (mm)
Drift length	300	Drift length	360
Matching quadrupole MQ1	200	Dipole D2 ρ = 50cm, θ = 60º	500
Drift length	100	Drift length	1240
Matching quadrupole MQ2	200	Focus quadrupole FQ2	240
Drift length	300	Drift length	60
Focus sextupole FS1	120	Focus sextupole FS2	120
Drift length	60	Drift length	60
Focus quadrupole FQ1	240	Focus sextupole FS2	120
Drift length	1240	Drift length	300
Dipole D1 ρ = 50cm, θ = 60º	500	Matching quadrupole MQ3	200
Drift length	360	Drift length	100
Multipole M	240	Matching quadrupole MQ4	200
Drift length	360	Drift length	300

TECHNICAL DETAILS OF BENDING AND FOCUSSING ELEMENTS

Table 2.Technical specifications of electrostatic elements

Electrostatic element	Length (mm)	Diameter (0m)	Maximum voltage (V)	Voltage tolerance (V)	Quantity
Matching quadrupole MQ	200	40	1000	± 1	4
Focus quadrupole FQ	240	80	1000	± 1	2
Focus sextupole FS	120	40	100	± 1	2
Multipole M:	240	400			1
Sextupole			500	± 1	
Octupole			20	± 1	
Decapole			2	± 1	
Dodecapole			2	± 1	

Table 3. Technical specification of bending dipoles

Angle (°)	Radius (mm)	Pole gap (mm)	Pole width (mm)	Entrance Angle (°)	Exit Angle (°)	Weight (Kg)	Power (kW)	Coolant flow (1/min)	Coolant pressure (bar)	Quantity
60	500	80	620	23	23	5600	15	11	3-5	2

The calculated ion optics is shown in Figure 2 and Figure 3. The ion-optical code COSY INFINITY [1] was used for these calculations. The phase space dimensionality used was 2, being the x-a as well as y-b motion computed. Kinetic energy, mass and charge are calculated as parameters and thus all calculations are performed in the following scaled coordinates:

[1] = x, [2] = a = p_x/p_0, [3] = y, [4] = b= p_y/p_0,

[5]=$\delta_K=(K-K_0)/K_0$, [6]=$\delta_m=(m-m_0)/m_0$, [7]=$\delta_Z=(z-z_0)/z_0$

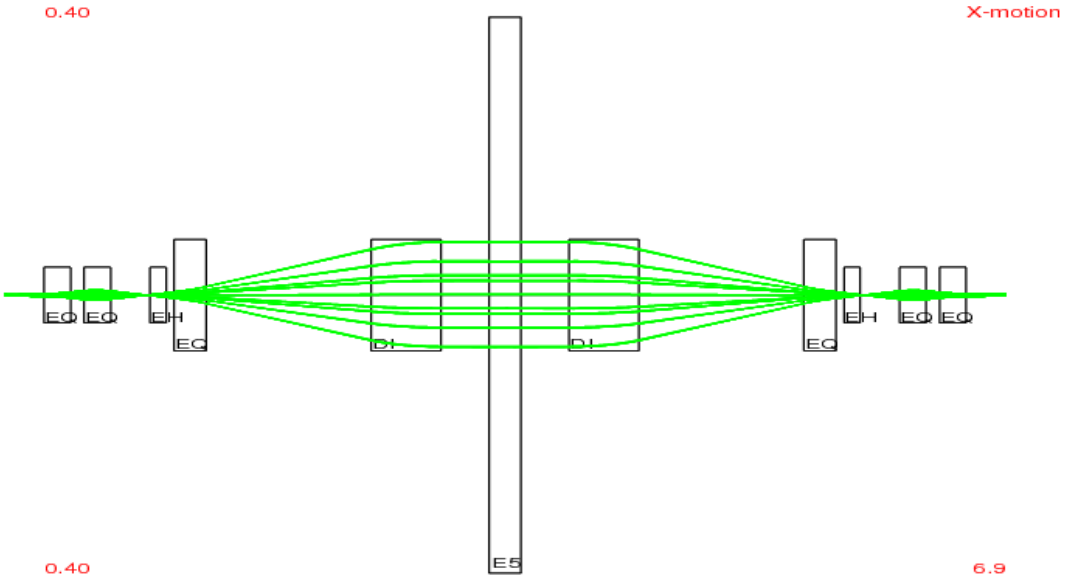

Figure 3. Beam envelop calculation for the x direction. The beam emittance at the entrance is supposed to be 1 mm mrad.

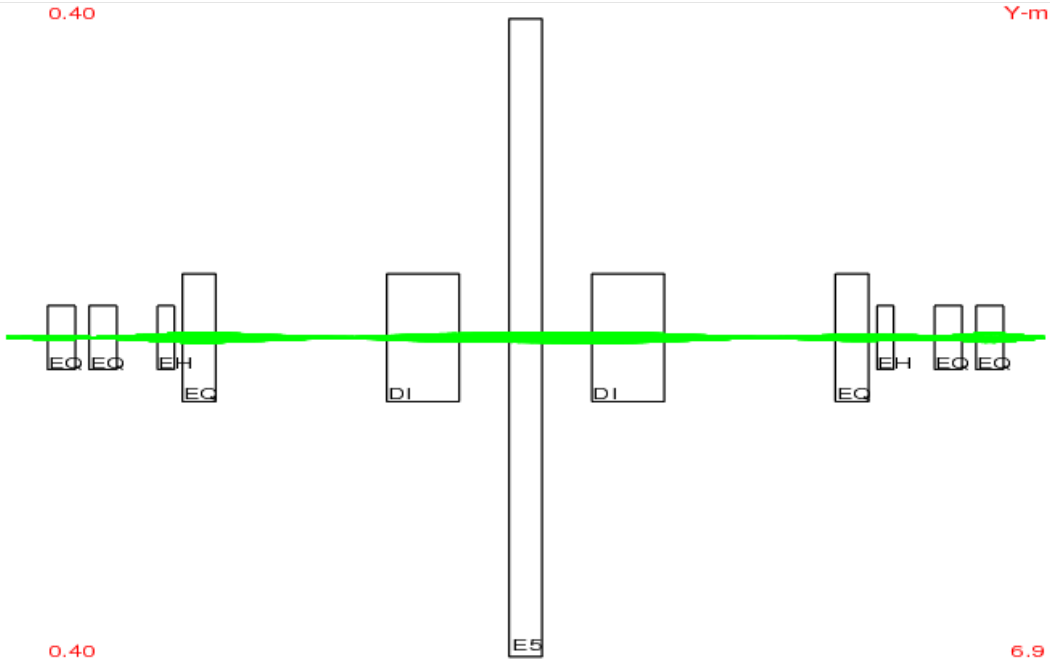

Figure 4. Beam envelop calculation for the y direction. The beam emittance at the entrance is supposed to be 1 mm mrad.

FOCUSSING CONDITIONS

Focussing and corrective elements are all electrostatic and so settings are independent of mass. The different focussing conditions are detailed below.

- Quadrupole doublet:

  The doublet consist of a pair of quadrupoles of opposite polarity MQ1~ -0.76 V and MQ2~0.90 V, and separated by a drift distance L=10cm which is small compared to the focal length of the individual quadrupoles. This matching section produces a ribbon-shaped beam, with (x,x)=-0.19, (y,y)=-3.4. The full first order transfer matrix at L=20cm after the doublet is given below.

	(x,)	(a,)	(y,)	(b,)	(t,)	
x	-0.1933524	-11.39821	0.000000	0.000000	0.000000	100000000
a	**-0.6787594E-08**	-5.171904	0.000000	0.000000	0.000000	010000000
y	0.000000	0.000000	-3.420909	-10.04023	0.000000	001000000
b	0.000000	0.000000	**0.6802835E-07**	-0.2923197	0.000000	000100000

  The different columns of the transfer matrix correspond to the final coordinates *x, a, y, b* and *t*, where *t* is the time-of-flight. The lines contain the various expansion coefficients. The last column indicates the corresponding expansion coefficient, so that *100000000* in the first row means (x,x) = -0.1933524, (a,x)= -0.1933524, (y,x) = 0, (b,x)

=0, and (t,x) = 0. The same for the following rows, i.e. (x,a) = -0.6787594E-08, (a,a) = -5.171904, etc.

The focus condition is point-to-point in both x and y so that (x,a)=0 and (y,b)=0

- Third quadrupole :

The third quadrupole with negative polarity and magnitude Q1~ -1.155V, diverges in x-direction and converges in y-direction. The first order transfer matrix just in front the first dipole is given by

	(x,)	(a,)	(y,)	(b,)	(t,)	
x	**-40.27679**	-26.45579	0.000000	0.000000	0.000000	100000000
a	-17.80091	-11.71735	0.000000	0.000000	0.000000	010000000
y	0.000000	0.000000	4.706484	8.923750	0.000000	001000000
b	0.000000	0.000000	-0.1082218	**0.7278220E-02**	0.000000	000100000

The large x area in the dipoles gives mass dispersion. The small y size minimise y aberrations and the small y-angles minimise b aberrations.

- Mid-plane:

The focusing condition at the mid-plane is (a,a)=(y,b)=(b,y)=0, so point-to-parallel in x, and point-to-point/parallel-to-parallel in y. The first order transfer matrix at the mid-plane is given by

	(x,)	(a,)	(y,)	(b,)	(t,)	
x	-46.38150	0.489476E-01	0.000000	0.000000	0.000000	100000000
a	-20.52008	**0.950677E-04**	0.000000	0.000000	0.000000	010000000
y	0.000000	0.000000	7.619594	**0.486093E-02**	0.000000	001000000
b	0.000000	0.000000	**-0.686620E-04**	0.1312405	0.000000	000100000
δe	**0.3838987**	0.5391315	0.000000	0.000000	0.000000	000000100
δm	**0.3838985**	0.5391313	0.000000	0.000000	0.000000	000000010
δz	**-0.7677972**	-1.078263	0.000000	0.000000	0.000000	000000001

As a pure magnetic separator, the dipole disperses ions according to their rigidity, and then, the mass and energy dispersions are equivalent and equal to half of the momentum dispersion D_P. The calculated D_P is ~0.77 cm/% and the corresponding energy and mass dispersion is ~0.38 cm/%. The charge dispersion D_Z is equal to $-D_P$.

- Final focus:

Mirror symmetry is exploited so that some of the coefficients in the transfer map will vanish. As a consequence the reverse section transforms the ribbon-shaped beam back to a circular cross section at the focal plane. The final first order transfer matrix is

-1.000062	-4.520500	0.000000	0.000000	0.000000	100000000
-0.2733026E-06	**-0.9999380**	0.000000	0.000000	0.000000	010000000

0.000000	0.000000	**0.9999645**	0.7517624E-01	0.000000	001000000
0.000000	0.000000	-0.2266671E-08	**1.000034**	0.000000	000100000
-22.12742	-50.01247	0.000000	0.000000	0.000000	000000100
-22.12741	-50.01244	0.000000	0.000000	0.000000	000000010
44.25483	100.0249	0.000000	0.000000	0.000000	000000001

The final mass dispersion is D_m ~22 cm/% which will allow one to obtain a maximum mass resolution of ~20000 for a beam of 1π mm mrad emittance. The full system is focusing point-to-point in both *x* and *y*, so that (x,a)=(y,b)=0 and parallel-to-parallel in *y* so that (b,y)=0. The system is symmetric in *y* so that magnifications (y,y)=(b,b)=1, and mirror symmetric in x, so (x,x)=(a,a)=-1.

Higher order aberrations:

All non-zero non-linear terms blur the final image and reduce the resolving power. Sextupoles allow correcting second order aberrations. Its first order transfer matrix is that of a drift space and so does not affect the first-order optics of the beam line. However, the presence of more than one sextupole in the beam line may induce significant third or higher order aberrations and as a consequence multipole elements should be included (sextupole, octupole, decapole and duodecapole) to correct the induced higher order effects.

MASS SPECTRUM SIMULATIONS

A Monte Carlo code has been developed to calculate the mass distributions transformed through the COSY INFINITY 5th order transfer matrix. The transfer matrixes are read by the Monte Carlo code as ASCII files, and as a consequence, a large number of particles can be transformed through the transfer matrix, avoiding the intrinsic limitations of the COSY code for tracing rays.

The initial beam phase space was assumed to be elliptic and Gaussian with FWHM values Δx = 1mm and Δa = 12mrad. The final position of each particle is calculated as the sum of all aberrations.

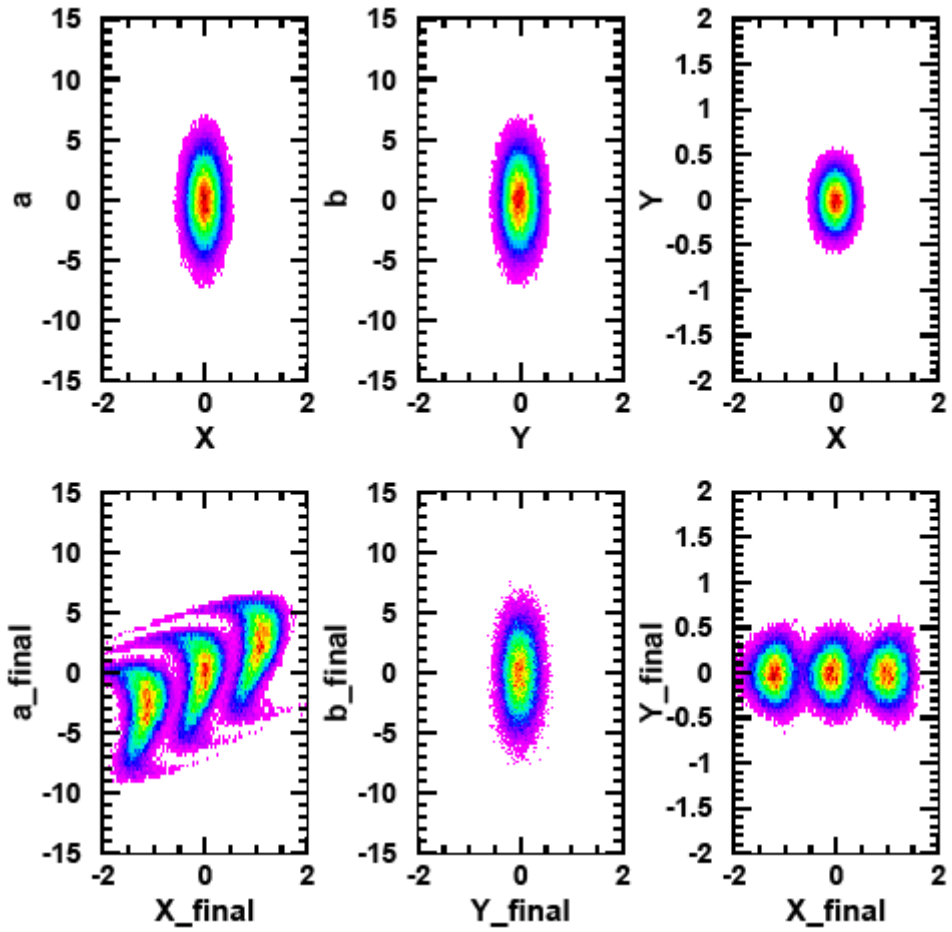

Figure 5.Top panel: initial beam phase space used in the Monte Carlo code. The phase space was assumed to be elliptic and Gaussian with FWHM values Δx = 1mm and Δa = 12mrad. The left upper panel represents x-a phase space, the middle panel the y-b phase space, and the right panel the x-y plane at the entrance of the HRS. Bottom panel: calculated phase space distributions at the final focal plane of the HRS. 50000 particles are transformed through the 5th order transfer matrix calculated by COSY INFINITY. The particles have the mass deviations -1/20000, 0 and +1/20000.

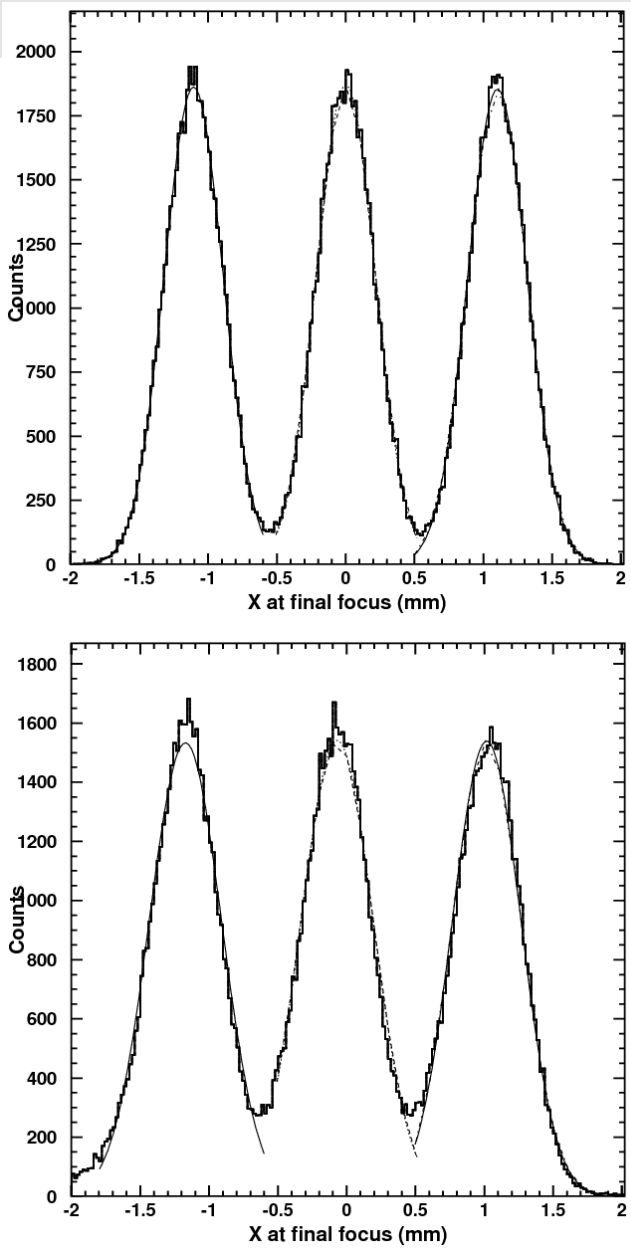

Figure 6. Mass separation spectrum as calculated by the Monte Carlo Code at the final focal plane of the HRS. 50000 particles with mass deviations -1/20000, 0, and +1/20000 were transformed through the first order (top) and fifth order (bottom) transfer matrix as calculated by COSY INFINITY. The initial phase space was assumed to be elliptic and Gaussian with FWHM values Δx = 1mm and Δa = 12mrad

ALIGNMENT EFFECTS

The next step in the study of the separator performance is computing the aberrations due to mechanical imperfection or misalignments. The results from this study can be used for the estimation of tolerance limits on the precision of machining and alignment of the different optical elements in the separator. COSY INFINITY was used to calculate the coordinate change due to misalignments errors through the separator, to find tolerances on various lens elements. The Monte Carlo code has been used to observe the blur in mass separation. The advantage of using COSY INFINITY is that the higher order transport matrix can be easily read into the Monte Carlo code, and consequently a large number of particles can be transformed through the transfer matrix.

The resolving power is given by

$$R = \frac{(x \mid \delta m)}{2x_f}$$

where $(x \mid \delta m)$ is the first order mass dispersion matrix element and $2x_f$ is the final beam diameter.

The resolving power can be redefined by introducing the mass dispersion obtained from the MonteCarlo simulations, so that

$$R^* = \frac{\Delta x}{\delta m \cdot 2x_f}$$

where Δx is the total 5^{th} order mass dispersion calculated by fitting the simulated mass distribution and δm is the mass deviation introduced in the simulation.

In the following the effect of misalignments of the different beam line elements is show.

SHIFT OF THE OPTIC AXIS

THE TRANSVERSE DISPLACEMENT

QUADRUPOLES:

The electrostatic field symmetry in the quadrupoles with respect to the xOz plane is preserved, so that transverse misalignments in the dispersive x-direction do not have any influence in the y-direction. However, a misalignment in the y-direction introduces aberrations in the y-direction but also transverse misalignments exits in the x-direction which affects higher order terms in the transfer matrix. The same effect is observed when the optic axis is tilted by a given angle. If the axis is tilted by an angle in the x-direction, only transverse x-displacements are observed, however a tilt in the optic axis in y-direction affects both x- and y-positions at the focal plane. The calculated shifts in positions and final resolving powers calculated for the different beam line elements are summarised in the tables below.

Table 4. MQ1

SHIFT (mm)	Offset (mm)	$2x_f$ (mm)	Δx (mm)	R	R*
0.1	0.23294	1.1961	1.0900	18489	18226
0.2	0.54118	1.2237	1.0972	18071	17933
0.3	0.85295	1.1888	1.0918	18602	18369
0.4	1.16295	1.2065	1.0946	18329	18145
0.5	1.47607	1.1813	1.0962	18720	18559
1.0	3.03338	1.25948	1.0849	17558	17227

Table 5. MQ2

SHIFT (mm)	Offset (mm)	$2x_f$ (mm)	Δx (mm)	R	R*
0.1	-0.9950	1.1893	1.0979	18594	18464
0.2	1.9097	1.2407	1.0961	17824	17669
0.3	-2.8246	1.2754	1.0882	17339	17064
0.4	-3.7237	1.2752	1.087	17341	17047
0.5	-4.6278	1.2956	1.0811	17069	16689
1.0	-9.1340	1.9091	1.0449	11583	10947

Table 6. Q1

SHIFT (mm)	Offset (mm)	$2x_f$ (mm)	Δx (mm)	R	R*
0.1	-0.735	1.233	1.104	17933	17908
0.2	-1.385	1.230	1.099	17973	17862
0.3	-2.036	1.240	1.101	17841	17757
0.4	-2.692	1.309	1.105	16899	16885
0.5	-3.330	1.313	1.109	16840	16896
1.0	-6.510	1.498	1.104	14758	14741

DIPOLES:

Due to the symmetry in the magnetic field of the dipoles magnets, misalignments in the dispersive x-direction have produced only transversal displacements in the final x-position.

Table 7. DIPOLE 1

SHIFT (mm)	Offset (mm)	$2x_f$ (mm)	Δx (mm)	R	R*
0.1	1.17419	1.04791	1.1064	21103	21117
0.2	2.29200	1.41800	1.1150	15592	15719
0.3	3.51244	1.60647	1.1128	13766	13854
0.4	4.77260	1.63228	1.0960	13548	13429
0.5	6.03415	1.72200	1.1170	12838	12972

MULTIPOLE:

A misalignment in the x-direction almost does not shift the x-position of the final focal plane; however a shift of only 0.1mm begins to blur mass separation. This effect is due to the fact that the phase space x-a starts to deform, turning to the left, as can be seen in Figure 7.

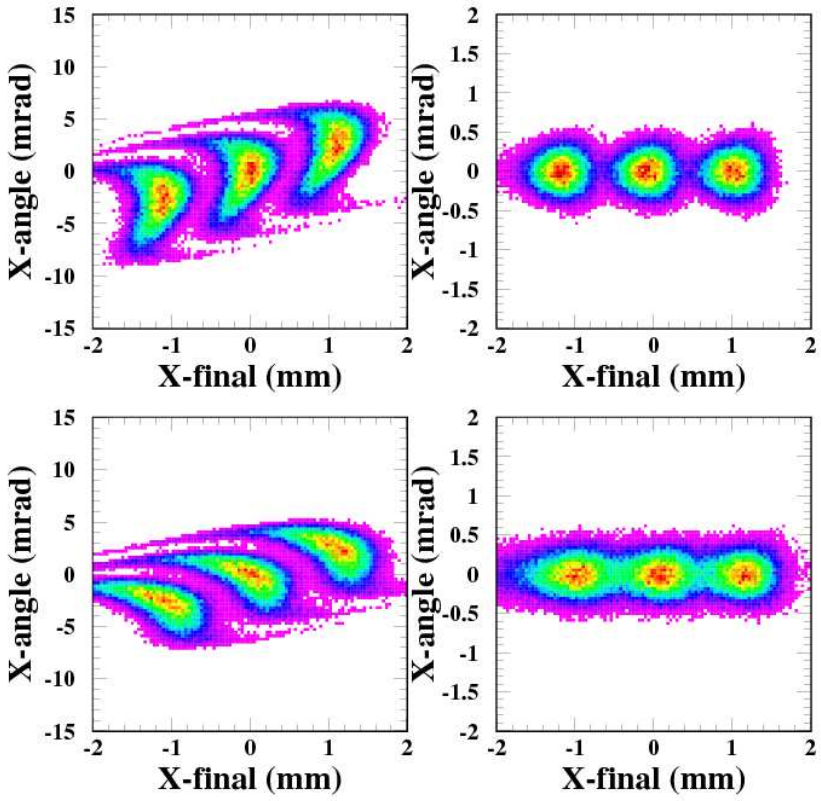

Figure 7 Top panel: x-a (left) and x-y (right) phase space at the final focal plane of the HRS for the designed ion optics. 50000 particles with mass deviations -1/20000, 0, and +1/20000 were transformed through the fifth order transfer matrix calculated by COSY INFINITY. Bottom panel: corresponding phase spaces for a shift of 0.2mm in the dispersive x-direction. As can be seen, the deformation in the x-a phase space is the responsible for the blur in the final mass separation.

Table 8. MULTIPOLE

SHIFT (mm)	Offset (mm)	$2x_f$ (mm)	Δx (mm)	R	R*
0.1	-0.015	1.238	1.076	17860	17377
0.2	0.086	1.884	1.051	11737	11156
0.3	0.185	3.703	1.002	5972	5409

SEXTUPOLES:

Calculations have been done for the focusing sextupoles, and it has been observed that offsets in the optical axis in x-direction introduce small shifts (~0.03 mm for 1mm shift) in the final x-position at the exit of the spectrometer. However, the transversal shifts introduce a tilt

in the phase space x-a, which have an important influence on the final resolving power, as can be seen in table 9.

Table 9. SEXTUPOLE

SHIFT (mm)	Offset (mm)	$2x_f$ (mm)	Δx (mm)	R	R*
0.1	-0.078	1.242	1.108	17804	17835
0.2	-0.077	1.269	1.111	17424	17505
0.3	-0.072	1.308	1.114	16907	17028
0.4	-0.058	1.303	1.116	16973	17135
0.5	-0.047	1.351	1.099	16366	16263
0.7	-0.008	1.511	1.121	14632	14840
1.0	0.073	1.733	1.116	12762	12877

MISALIGNING ALL ELEMENTS "RANDOMLY"

The effect of the simultaneous transversal misalignment of the different elements in the beam line was also studied. The results of the corresponding simulations are summarised in the table 10. As can be seen, the final resolution is reduced and the mass distributions at the final focal plane present an offset as shown in Figure 8, and the values given in the table 10.

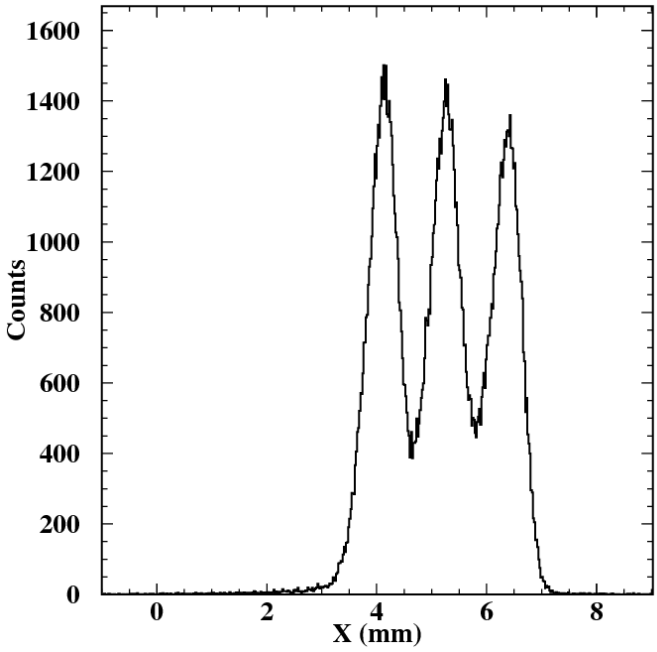

Figure 8. Effect in the mass distribution of the simultaneous transversal misalignment of the different elements in the beam line. 50000 particles with mass deviations -1/20000, 0, and +1/20000 were transformed through the fifth order transfer matrix calculated by COSY INFINITY. The figure corresponds to the data of the second row in table 10. The final resolution is reduced to ~17000 and the mass distributions at the final focal plane present an offset of +5.31 mm

Table 10: Fifth order effect of misalignment in different beam line elements in the resolving power. The shift in the different beam line elements is given in mm.

MQ 1	MQ 2	SX 1	Q1	D1	M	D2	Q2	SX 2	MQ 3	MQ 4	Offset (mm)	$2x_f$ (mm)	Δx (mm)	R	R*
0.5	-0.2	0.3	-0.3	0.2	0.1	-0.1	0.2	-0.1	-0.3	0.4	5.26	1.24	1.10	17829	17760
0.5	-0.2	0.3	-0.3	0.2	0.2	-0.1	0.2	-0.1	-0.3	0.4	5.31	1.30	1.08	16986	16613
0.2	0.4	-0.1	0.1	-0.2	0.3	0.4	-0.2	-0.5	0.2	-0.1	-3.12	2.80	0.96	7902	6887

THE ROTATION OF THE OPTICAL AXIS

The effect of the rotation of the optical axis was also studied for the different beam line elements. It was observed that for the focussing quadrupole, already a 1mrad skew produces a shift in the final focal plane of 1.9 mm. The sextupoles and multipole are essentially insensitive to the rotation of the axis. And finally, rotations in dipole magnets produce changes in the effective edges angles, which affect the final resolving power. The tables below show calculations corresponding to the focusing quadrupole, dipole and the multipole.

Table 11. Q1

skew (mrad)	Offset (mm)	$2x_f$ (mm)	Δx (mm)	R	R*
0.1	0.11274	1.22187	1.0992	18098	17991
0.4	0.68570	1.20274	1.1003	18386	18296
1.0	1.82938	1.20973	1.0972	18280	18139
2.0	3.72684	1.19452	1.0986	18513	18393

Table 12. D1

skew (mrad)	Offset (mm)	$2x_f$ (mm)	Δx (mm)	R	R*
0.1	0.18879	1.29885	1.1020	17026	16968
0.4	1.05172	1.48464	0.9301	14895	12530
0.6	1.67377	1.68677	1.1191	13110	13269
1.0	2.88650	1.85820	1.1064	11901	11908

Table 13.MULTIPOLE

skew (mrad)	Offset (mm)	$2x_f$ (mm)	Δx (mm)	R	R*
0.1	-0.078	1.221	1.098	18112	17988
0.5	-0.078	1.222	1.098	18100	17978
1.0	-0.078	1.222	1.098	18092	17970
1.5	-0.078	1.223	1.098	18089	17969
2.0	-0.078	1.223	1.098	18082	17962

Table 13 SEXTUPOLE

skew (mrad)	Offset (mm)	$2x_f$ (mm)	Δx (mm)	R	R*
0.1	-0.012	1.213	1.097	18225	18083
0.5	0.240	1.231	1.093	17971	17761
1.0	0.544	1.216	1.096	18179	18024
1.5	0.860	1.203	1.100	18389	18291
2.0	1.167	1.240	1.099	17835	17733

REFERENCES

[1] M. Berz, Nucl. Instr. and Meth. A 298 (1990) 473